Spring 6-16-2023

Consumer 3D Printing for Remote Control Aircraft Wings: Development of Novel Wingbox Structure

Ian Clark
Portland State University

CONSUMER 3D PRINTING FOR REMOTE CONTROL AIRCRAFT WINGS: DEVELOPMENT OF NOVEL WINGBOX STRUCTURE

by

Ian Clark

An undergraduate honors thesis submitted in partial fulfillment of the

requirements for the degree of

Bachelor of Science

in

University Honors

and

Mechanical Engineering

Thesis Advisor

Lemmy Meekisho

Portland State University

2023

CONSUMER 3D PRINTING FOR REMOTE CONTROL AIRCRAFT WINGS: DEVELOPMENT OF NOVEL WINGBOX STRUCTURE

Ian Clark[1]
[1]Portland State University, Portland, OR, United States

ABSTRACT

Remote control aircraft construction and can be a very expensive and time-consuming hobby. With 3D printer consumer adoption rates skyrocketing [3], there is a gap between demand for RC aircraft and suitable well-designed models available to creators and hobbyists. By creating and testing two iterations of wingbox geometries, this research aims to help close that gap by producing an easily printable wing structure. While there are improvements that can be made on this work, this research has been effective in generating a novel wingbox structure for FFF 3D printing that has distinct advantages over other designs currently available.

Keywords: Remote Control Airplane Wing, Wingbox, Additive Manufacturing, 3D Printing.

NOMENCLATURE

3D Printing	Manufacturing technology
FFF	'Fused Filament Fabrication'
PLA	'Polylactic Acid'
AM	'Additive Manufacturing'
Airfoil	Wing cross section or wing profile
Infill	Solidness of a 3D print
Layer Height	The height of each print layer
Wall line width	The thickness of a printed wall
RC	Remote Control

1. INTRODUCTION

3D Printing is an emerging technology with an increasing number of applications in the global supply chain. The utility of 3D printing for many applications is still limited by individual user's understanding of the technology [2] thus there are many niches and areas of industry where the technology has yet to meet its full potential.

Aircraft wingbox technology may be one such application. One advantage of the technology is the ability to form unique geometries into a single fused body. Major aerospace companies like Boeing have used 3D printing to transform complicated interior aircraft assemblies, such as complex tube networks, into prints, reducing costs and weight drastically.

Complicated wingbox structures have long been used to create wings for major aerospace and hobbyist applications. 3D printing has emerged as a viable alternative construction method in the remote control (RC) niche, where complicated subassemblies can be replaced with a single print. However, 3D printable RC aircraft models available today have poor structural integrity due to their fundamental design. They accommodate for this by having short wings or using carbon fiber spars to provide structural stability on long wings. Short wings reduce flight efficiency drastically, and while carbon fiber spars are effective, such a construction amounts to a carbon fiber spar wingbox with a 3D printed cover, which is not the same as a 3D printed wingbox.

The scope of this research is to assess the feasibility of an alternative design which uses a conventional thin film exterior and 3D printed grid structure. The goal is to develop a structurally sound and weight efficient structure which prints well on a fused filament 3D printer for hobbyist consumer applications.

Additive manufacturing gains wider adoption in manufacturing each year, and composites gain wider adoption in aerospace, as major companies like Boeing and Airbus implement widescale composite structures on their aircraft, such as the Boeing 787 Dreamliner. Additionally, large scale 3D printing robots are becoming a more commonplace technology. Ultimately, a 3D printed wingbox design could effectively fill a niche in consumer aerospace endeavors like RC aircraft, hang gliders, and fixed wing gliders, where the costs of manufacturing and assembly for complicated wing structures can dominate material costs.

2. METHODS

Destructive testing was used to determine the strength of sets of 3D printed wing sections. Each component is a standard wing shape and size, with unique internal structures. The wing profile is a slightly modified Clark Y profile, a common wing profile used in RC planes.

The objective of this project was to develop a wing structure, test it to failure in a full factorial experiment examining two controlled variables, subjectively analyze the mode of failure, design a modified structure which addressed failure modes and capitalized on factorial findings, and repeat. Ultimately, two wing designs, abbreviated as WD1 and WD2, were tested.

The test apparatus, figure 1, was used to load wings horizontally until static failure. The load was applied steadily and slowly. The highest reading on the scale observed by the tester before failure occurred was recorded as the static load at failure. Failure is defined here as brittle or ductile failure resulting in a full release of the wing from the apparatus.

FIGURE 1: TEST APPARATUS VERTICAL VIEW..

All structures were produced using fused filament fabrication on an Ender 3 3D printer. Settings kept constant were zero percent infill, layer height of 0.2 mm, wall thickness of 0.4 mm, nozzle and bed temperature of 200 degrees Celsius and 60 degrees Celsius respectively. A 0.4 mm nozzle was used. Overture PLA Professional plastic filaments of gray and white colors were used. The filament was stored in sealed Ziploc bags alongside 50 grams of silica gel desiccant when not in use.

First, a wing section, wing design 1, abbreviated WD1, was designed, modeled, and printed. WD1 is pictured in figure 2. A factorial experiment design was used to determine the key factors which affected the resistance to failure of WD1. Factors tested were spar thickness and number of walls printed. With k=2 factors, each run had n=4 runs, and 2 replicates were performed, with a total of 8 wing sections tested.

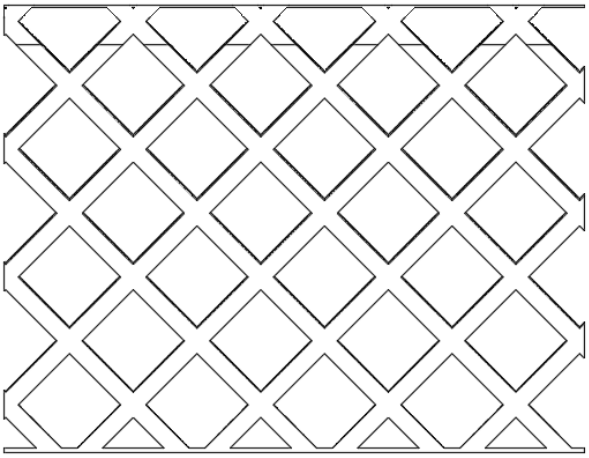

FIGURE 2: WD1.

Second, another wing design was tested, wing design 2, abbreviated as WD2. This design was an iteration of the first design based on the results of the first factorial experiment. This testing was done as a single point test, with one spar width changed between tests. The wings are pictured in figure 3.

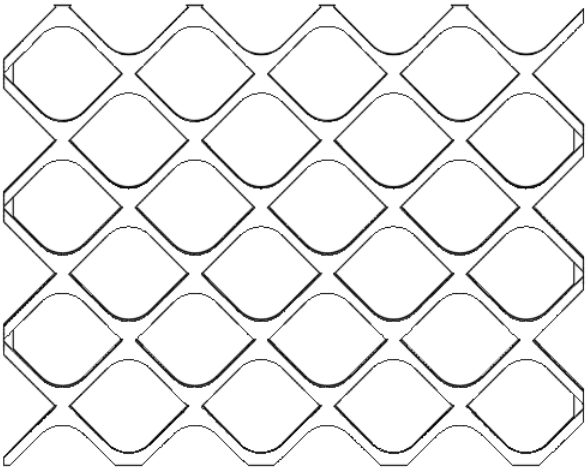

FIGURE 3: WD2.

A solid wall wing structure with 5% infill was printed to establish a baseline value for strength and allow strength to weight comparison. After WD2 was determined to be viable, it was used to fabricate a model aircraft for test flying, a drawing of which is pictured in figure 4.

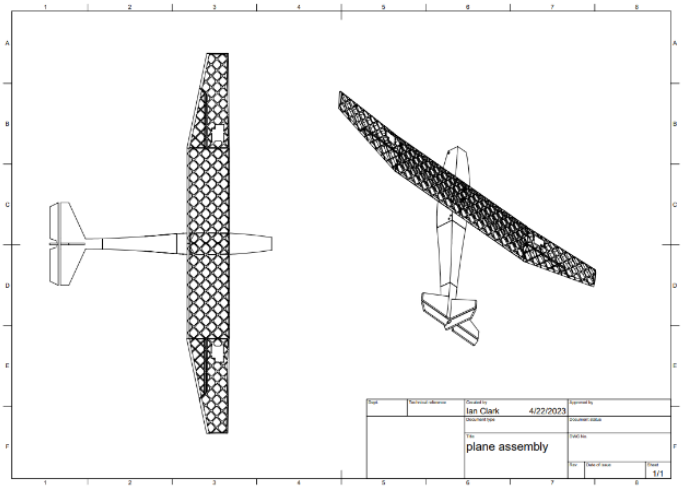

FIGURE 4: MODEL AIRCRAFT DESIGN DRAWINGS. WINGSPAN IS 0.9 METERS.

3. RESULTS AND DISCUSSION

Results of the first factorial experiment on WD1, table 1, show that wall thickness influences strength with high significance, and spar thickness does not significantly influence strength. The forces recorded at failure are tabulated in table 2. Figure 5 highlights the impact of spar width and number of walls on the break force.

TABLE 1: *RESULTS OF LINEAR REGRESSION ON FACTORIAL TEST.*

	Estimate	*Std. Error*	*t value*	*Pr(>|t|)*
Intercept	*-6.700*	*6.494*	*-1.032*	*.349517*
spar	*2.048*	*2.838*	*.722*	*.502901*
walls	*22.200*	*2.980*	*7.450*	*.000687*

TABLE 2: *PHYSICAL RESULTS FROM FACTORIAL EXPERIMENT ON WD1, WITH AVERAGE FORCE AT FAILURE.*

Model	No. Walls	Spar Thickness (mm)	Spar Width (mm)	Weight (g)	Failure Force (N)
WD1	1	1.05	4	5	15.7
WD1	1	2.1	4	6	18.6
WD1	2	1.05	4	6	43.2
WD1	2	2.1	4	9	44.6

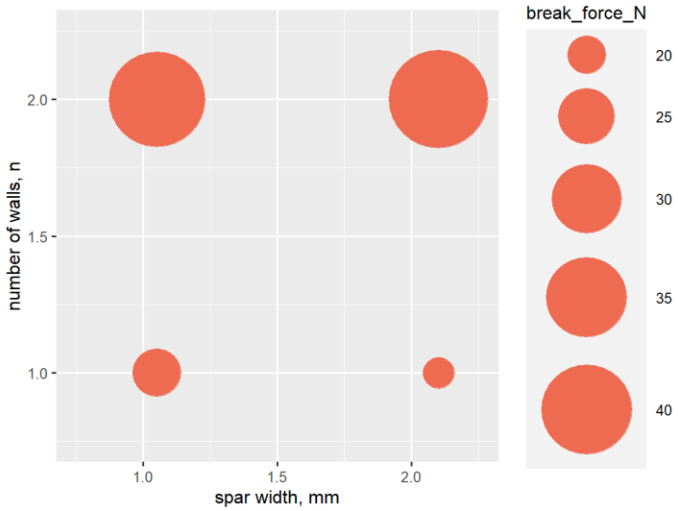

FIGURE 5: *SIZE PLOT OF WD1 BREAK FORCE FROM FACTORIAL EXPERIMENT.*

Failure analysis conducted on the first round of designs showed that failure occurred at the X shaped vertices where spars meet. Two causes were identified: less material and higher stress concentration at junctions.

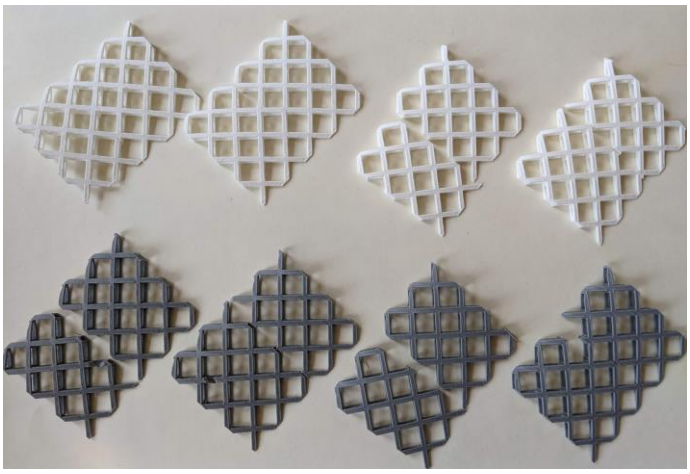

FIGURE 6: *WD1 AFTER FAILURE.*

The difference in the amount of material can be seen via cross section at these junctions, figure 7, which shows a solid model of wing geometry. However, when printed, the wing is a hollow shell of 0.4 mm (1 wall) or 0.8 mm (2 wall) thickness. A cross section at non-junction locations, figure 7b, shows approximately 4 times as much material resisting failure as compared to figure 7a.

Cause two is stress concentration. These intersections contain sharp 90° angles, which increase stress concentration [1] and reduce resistance to failure in loading. The results of this failure can be seen in fig. x in the methods section, where failure can be observed to occur exclusively at the intersections. The *stress concentration factor*, K_t, can be calculated using equation 1 [1]:

$$K_t = 2\left(\frac{a}{p_t}\right)^{.5} \quad (1)$$

Where a is the length of the surface crack, and p_t is the radius of curvature of the crack tip. Calculation reveals an approximate stress concentration factor at junctions for WD1 of $K_t = 25.29$.

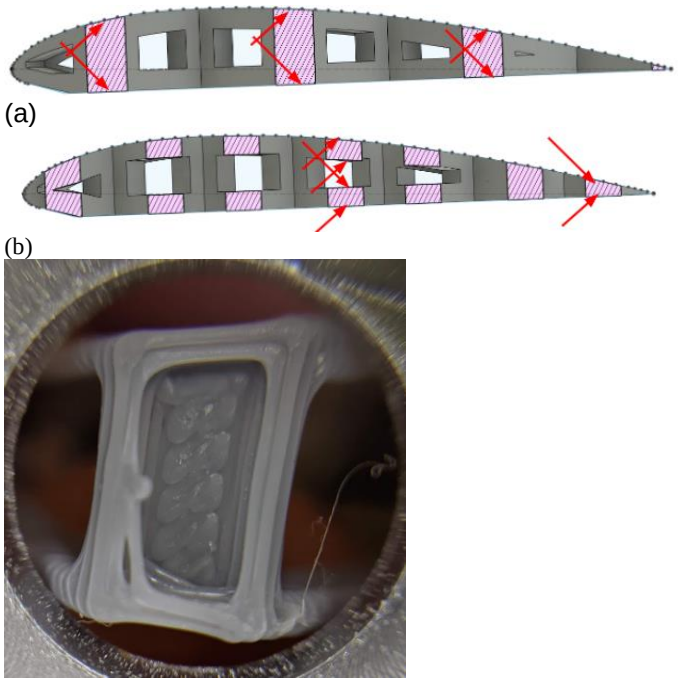

FIGURE 7: *CROSS SECTIONS OF WD1 ON (a) JUNCTIONS AND (b) SPARS AND (c) PHYSICAL CROSS SECTION OF 2 WALL WD1 AT JUNCTION.*

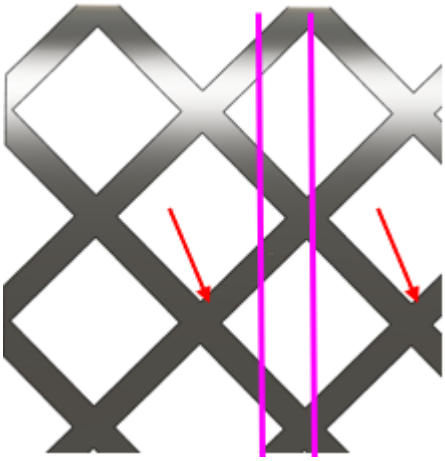

FIGURE 8: *VERTICAL VIEW WD1 SUBSECTION, CRACK PROPAGATION FAILURE POINTS HIGHLIGHTED WITH RED ARROWS. CROSS SECTIONS HIGHLIGHTED WITH PINK LINES.*

A second iteration wing design, WD2, was generated to eliminate or minimize these failure points by replacing the sharp

90° angle with a rounded fillet. The stress concentration after this change was reduced to approximately K_t = 2.35, a 1076% decrease in stress concentration.

WD2 also increases the amount of material resisting failure at junctions, demonstrated in figure 9. Figure 9c can be compared directly with figure 7c to see the improvement. This design was failure tested to assess the merit of the changes. Table 3 shows the results of this testing.

(a)

(b)

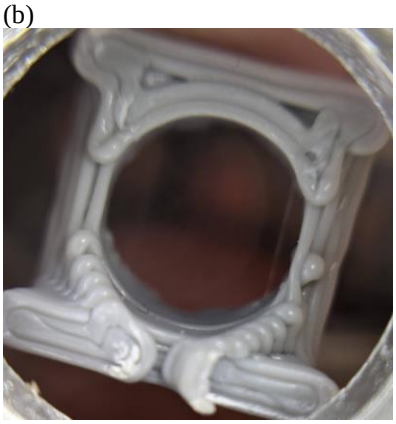

(c)

FIGURE 9: *(a) CROSS SECTION OF WD2 AT JUNCTIONS, AND (b) CROSS SECTION OF WD2 ON SPARS, AND (c) PHYSICAL CROSS SECTION OF 2 WALL WD2 AT JUNCTION.*

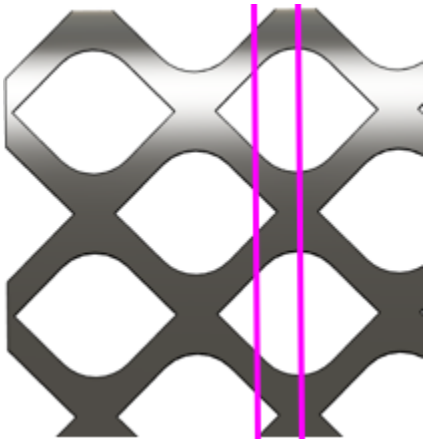

FIGURE 10: *VERTICAL VIEW OF WD2 SUBSECTION, CROSS SECTIONS SHOWN WITH PINK VERTICAL LINES.*

TABLE 3: PHYSICAL RESULTS FROM SOLID AND WD2 FAILURE TESTING

Model	No. Walls	Spar Thickness (mm)	Spar Width (mm)	Weight (g)	Failure Force (N)
Solid	2	N/a	N/a	14	200
WD2	2	1.4	1.4	5	43.2
WD2	2	1.4	2.8	8	91.8

4. Flight Testing

After testing revealed WD2 as a feasible wing structure, a model aircraft was printed and assembled using WD2. The model is pictured in figure 11.

FIGURE 11: *MODEL AIRCRAFT USING WD2.*

The aircraft saw a total of 3 flights and 3 crashes before a vertical nosedive caused irreparable damage to the structure of the aircraft. Pilot error is identified as the primary cause of the accident. Additionally, the craft may have been tail heavy. Throughout these 3 flights, the wing structure demonstrated its ability to support the flight loads of the aircraft sufficiently, and the ability to fly. Additionally, the wing survived multiple crashes with only minor damage, which was easily repairable with superglue. In the final crash, one half of the wing even survived the obliteration of the aircraft, pictured in figure 12.

FIGURE 12: *FINAL LANDING.*

The structure of the wing exceeded expectations and fulfilled its purpose. In the future, a slower moving, easier to control aircraft could be constructed to better demonstrate the performance of the wing and create a better flying experience.

5. Conclusion

WD2 has a feasible strength to weight ratio. It can be printed on most FFF printers with most types of material. It involves novel design elements and geometry which improve performance and weight savings over other designs in the RC space.

However, the design has its drawbacks. For one, it requires a film or covering to be adhered over the wing, which increases complexity of fabrication over a standard print which includes a wing shell. Additionally, the printing of this requires a heavy number of retractions, which is laborious for a printer, and causes stringing defects of certain filament, specifically the lightweight filament used for fabrication.

Most wings in the RC space use some combination of composite materials, layers of tape, superglue or cyanoacrylate glue, or carbon fiber spars to create sleek, strong, and durable wingbox geometries. To improve the focus and specificity of this study, we focused only on the fabrication of the wingbox using exclusively 3D printing. This means there are areas for immediate and significant improvement in the strength and durability of the wing. Processes such as using a carbon fiber spar along the length of the wing, coating the bottom of the wing in cyanoacrylate glue or superglue, or using a rigid tape along the length of the underside of the wing, would immediately improve strength drastically but were intentionally avoided for the purposes of this study.

An additional direction for further research would be in topological optimization. While this wingbox aims to be a suitable and competitive structure for an RC plane, hand calculations, and engineering principles, and design of experiments were used to optimize the geometry. Programs exist which can optimize the geometry of a structure based solely on user defined loadings and constraints, which could possibly be applied to this field to create a more ideal structure for loading distribution.

ACKNOWLEDGEMENTS

I would like to acknowledge the support of Dr. Meekisho of the Mechanical and Materials Engineering Department, who has been kind enough to volunteer his time to review and guide progress in this project.

BIBLIOGRAPHY

[1] William D. Callister Jr., and David G. Rethwisch, 2000, Materials Science and Engineering: An Introduction, John Wiley & Sons, NY.

[2] Snyder T.J., Andrews M., Weislogel M., Moeck P., Stone-Sundberg J., Birkes D., Hoffert M.P., Lindeman A., Morrill J., Fercak O., Friedman S., Gunderson J., Ha A., McCollister J., Chen Y., Geile J., Wollman A., Attari B., Botnen N., Vuppuluri V., Shim J., Kaminsky W., Adams D., Graft J., 2014 “3D Systems ’ Technology Overview and New Applications in Manufacturing, Engineering, Science, and Education,” Marry Anne Libert Inc. Vol. 1 No. 3 pp. 170-176, DOI 10.1089/3dp.2014.1502.

[3] Steenhuis, H-J., Pretorius, L., 2016, “Consumer additive manufacturing or 3D printing adoption: an exploratory study,” Journal of Manufacturing Technology Management, Vol. 27 No. 7, pp. 990-1012. DOI 10.1108/JMTM-01-2016-0002.

APPENDIX
ENGINEERING ANALYSIS:

Summary Section

The goal of a wingbox is to provide high resistance to failure at a light weight. High stress concentrations throughout the structure of the wing will lower the effectiveness of the wingbox. How much does this 90-degree angle increase stress concentrations at junctions, and how much could we reduce it by adding a fillet?

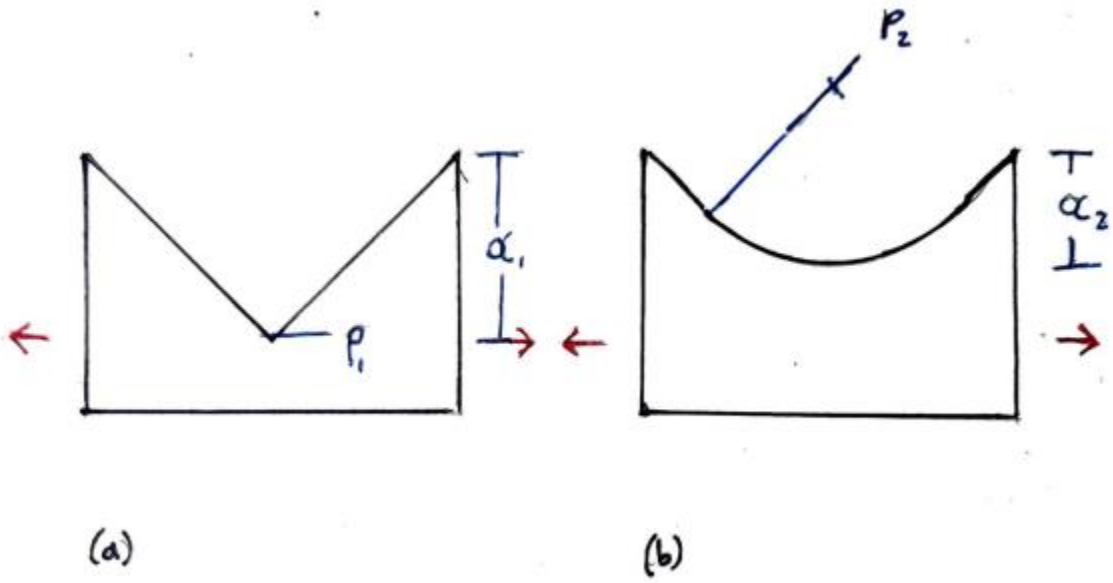

Results

The results of this calculation show that adding a fillet of radius 4.5mm will reduce the stress concentration at the point from 25.29x to 2.347x, a reduction of 1077.5% in stress concentration. This shows that this is probably a very effective step towards improving the effectiveness of the device, but that there is still room for improvement.

Evaluation

This calculation assumes orthogonal forces to the crack, as proposed in the diagram. However, the true forces are likely coming from an angle, and are not purely orthogonal to the crack. Additionally, geometric irregularities in the form of small cracks and imperfections induced on the geometry in the printing process pose the possibility of having a significant effect on the true stress concentration at failure points. However, this calculation provides a good guideline for the approximate size of fillet which would be appropriate, and it's sufficient for this design purpose.

Formulation Section

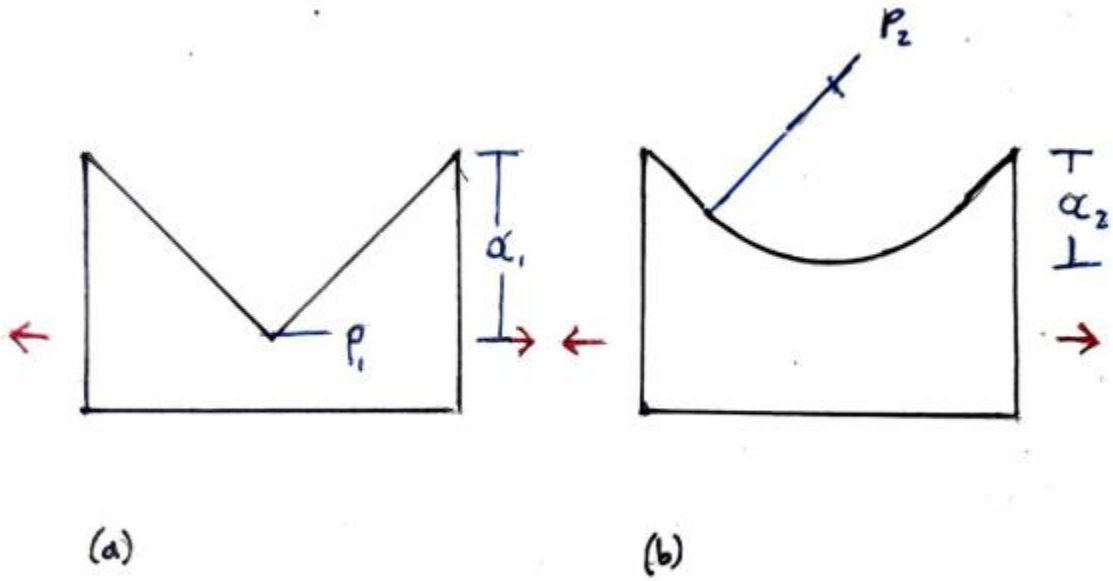

Given

Crack tip radius	p_1 = .05mm	p_2 = 4.5mm
Crack length	α_1 = 8.0mm	α_2 = 6.2mm

Find

1. Stress concentration in case (a) and case (b).
2. Change induced by adding a fillet.

Assumptions

1. The system can be modeled as a crack stress concentration.
2. Negligible concentration effect from layer lines and print imperfections.

Solution

$$K_t = 2\left(\frac{a}{p_t}\right)^{.5}$$

$$K_{ta} = 2\left(\frac{a}{p_t}\right)^{.5} = 2\left(\frac{8}{.05}\right)^{.5} = 25.29$$

$$K_{tb} = 2\left(\frac{a}{p_t}\right)^{.5} = 2\left(\frac{6.2}{4.5}\right)^{.5} = 2.347$$

$$\%change = \left(\frac{K_{t1}}{K_{t2}}\right) * 100\% = \left(\frac{25.29}{2.347}\right) * 100\% = 1077.5\%\ reduction$$

A) Clark Y Airfoil Coordinates

```
CLARK Y AIRFOIL
      61.0      61.0

 0.0000000 0.0000000
 0.0005000 0.0023390
 0.0010000 0.0037271
 0.0020000 0.0058025
 0.0040000 0.0089238
 0.0080000 0.0137350
 0.0120000 0.0178581
 0.0200000 0.0253735
 0.0300000 0.0330215
 0.0400000 0.0391283
 0.0500000 0.0442753
 0.0600000 0.0487571
 0.0800000 0.0564308
 0.1000000 0.0629981
 0.1200000 0.0686204
 0.1400000 0.0734360
 0.1600000 0.0775707
 0.1800000 0.0810687
 0.2000000 0.0839202
 0.2200000 0.0861433
 0.2400000 0.0878308
 0.2600000 0.0890840
 0.2800000 0.0900016
 0.3000000 0.0906804
 0.3200000 0.0911857
 0.3400000 0.0915079
 0.3600000 0.0916266
 0.3800000 0.0915212
 0.4000000 0.0911712
 0.4200000 0.0905657
 0.4400000 0.0897175
 0.4600000 0.0886427
 0.4800000 0.0873572
 0.5000000 0.0858772
 0.5200000 0.0842145
 0.5400000 0.0823712
 0.5600000 0.0803480
 0.5800000 0.0781451
 0.6000000 0.0757633
 0.6200000 0.0732055
 0.6400000 0.0704822
 0.6600000 0.0676046
 0.6800000 0.0645843
 0.7000000 0.0614329
 0.7200000 0.0581599
 0.7400000 0.0547675
 0.7600000 0.0512565
 0.7800000 0.0476281
 0.8000000 0.0438836
 0.8200000 0.0400245
 0.8400000 0.0360536
 0.8600000 0.0319740
 0.8800000 0.0277891
 0.9000000 0.0235025
 0.9200000 0.0191156
 0.9400000 0.0146239
 0.9600000 0.0100232
 0.9700000 0.0076868
 0.9800000 0.0053335
 0.9900000 0.0029690
 1.0000000 0.0005993

 0.0000000 0.0000000
 0.0005000 -.0046700
 0.0010000 -.0059418
 0.0020000 -.0078113
 0.0040000 -.0105126
 0.0080000 -.0142862
 0.0120000 -.0169733
 0.0200000 -.0202723
 0.0300000 -.0226056
 0.0400000 -.0245211
 0.0500000 -.0260452
 0.0600000 -.0271277
 0.0800000 -.0284595
 0.1000000 -.0293786
 0.1200000 -.0299633
 0.1400000 -.0302404
 0.1600000 -.0302546
 0.1800000 -.0300490
 0.2000000 -.0296656
 0.2200000 -.0291445
 0.2400000 -.0285181
 0.2600000 -.0278164
 0.2800000 -.0270696
 0.3000000 -.0263079
 0.3200000 -.0255565
 0.3400000 -.0248176
 0.3600000 -.0240870
 0.3800000 -.0233606
 0.4000000 -.0226341
 0.4200000 -.0219042
 0.4400000 -.0211708
 0.4600000 -.0204353
 0.4800000 -.0196986
 0.5000000 -.0189619
 0.5200000 -.0182262
 0.5400000 -.0174914
 0.5600000 -.0167572
 0.5800000 -.0160232
 0.6000000 -.0152893
 0.6200000 -.0145551
 0.6400000 -.0138207
 0.6600000 -.0130862
 0.6800000 -.0123515
 0.7000000 -.0116169
 0.7200000 -.0108823
 0.7400000 -.0101478
 0.7600000 -.0094133
 0.7800000 -.0086788
 0.8000000 -.0079443
 0.8200000 -.0072098
 0.8400000 -.0064753
 0.8600000 -.0057408
 0.8800000 -.0050063
 0.9000000 -.0042718
 0.9200000 -.0035373
 0.9400000 -.0028028
 0.9600000 -.0020683
 0.9700000 -.0017011
 0.9800000 -.0013339
 0.9900000 -.0009666
 1.0000000 -.0005993
```

B) RStudio Code for achieving results of factorial test on WD1.

```
library(corrplot)
library(ggplot2)
library(ggalley)

data <- read.csv("Thesisrunsfact.csv")
data
lmThesis <- lm(break_force ~ spar + walls, data=data)
lmThesis
summary(lmThesis)
```

C) Thesisrunfact.csv - factorial data set used for factorial test on WD1.

run	Force (N)
1	15.7
2	18.6
3	43.2
4	44.6
5	22.5
6	18.1
7	33.6
8	42.3